Exploration of O((r/R)^2) solution space for direct construction method

Jack Schroeder

Wistell meeting, Dec 12, 2019

Outline

- Overview of Landreman/Sengupta direct construction tool^{1,2,3}
- Optimization on input parameters solutions near a found minimum
- Direct parameter scan around minimum

^{1:} Direct construction of optimized stellarator shapes. I. Theory in cylindrical coordinates, Landreman, Sengupta, 2018, J Plasma Physics

^{2:} Direct construction of optimized stellarator shapes. II. Numerical quasisymmetric solutions, Landreman, Sengupta, Plunk, 2018, J Plasma Physics

^{3:} Constructing stellarators with quasisymmetry to high order, Landreman, Sengupta, 2019, J Plasma Physics

Why work with direct construction tool?

- Conventional optimization is slow, and highly dependent on good initial guess of boundary shape
- Direct construction from Garren & Boozer^{1,2} near axis expansion framework has advantages over optimization:
 - Could produce QHS solutions inaccessible to STELLOPT/ROSE
 - Rapid evaluation of the Fortran code (~10ms per solution) allows for efficient search of space of quasisymmetric solutions
- This semester I investigated the solution space around optimized solutions to access how to best use this tool in search of good QHS solutions

Direct construction tool overview

Algorithm based on Garren & Boozer^{1,2} near axis expansion:

$$r(r, \vartheta, \varphi) = r_0(\varphi) + X(r, \vartheta, \varphi)n(\varphi) + Y(r, \vartheta, \varphi)b(\varphi) + Z(r, \vartheta, \varphi)t(\varphi)$$

where t, n, b are vectors in Frenet-Serret frame of magnetic axis

$$rac{darphi}{d\ell}rac{doldsymbol{r}_0}{darphi}=oldsymbol{t}, \qquad rac{darphi}{d\ell}rac{doldsymbol{t}}{darphi}=\kappaoldsymbol{n}, \qquad rac{darphi}{d\ell}rac{doldsymbol{n}}{darphi}=-\kappaoldsymbol{t}+ auoldsymbol{b}, \qquad rac{darphi}{d\ell}rac{doldsymbol{b}}{darphi}=- auoldsymbol{n}$$

 expansion quantities further expanded as power series in inverse aspect ratio (major radius normalized to 1)

$$X(r, \vartheta, \varphi) = rX_1(\vartheta, \varphi) + r^2X_2(\vartheta, \varphi) + r^3X_3(\vartheta, \varphi) + \dots$$

$$B(r, \vartheta, \varphi) = B_0(\varphi) + rB_1(\vartheta, \varphi) + r^2B_2(\vartheta, \varphi) + r^3B_3(\vartheta, \varphi) + \dots$$

and first and second order terms are further expanded as follows:

$$X_1(\vartheta,\varphi) = X_{1s}(\varphi)\sin(\vartheta) + X_{1c}(\varphi)\cos(\vartheta),$$

$$X_2(\vartheta,\varphi) = X_{20}(\varphi) + X_{2s}(\varphi)\sin(2\vartheta) + X_{2c}(\varphi)\cos(2\vartheta)$$

Direct construction tool: quasisymmetry to first order

Algorithm based on Garren & Boozer^{1,2} near axis expansion:

$$r(r, \vartheta, \varphi) = r_0(\varphi) + X(r, \vartheta, \varphi)n(\varphi) + Y(r, \vartheta, \varphi)b(\varphi) + Z(r, \vartheta, \varphi)t(\varphi)$$

To first order in r, quasisymmetric fields are given by

$$r(r, \vartheta, \varphi) = r_0(\varphi) + \frac{r\bar{\eta}}{\kappa(\varphi)}\cos\vartheta n(\varphi) + \frac{rs_\psi s_G \kappa(\varphi)}{\bar{\eta}}\left[\sin\vartheta + \sigma(\varphi)\cos\vartheta\right] b(\varphi) + O(r^2/\mathcal{R})$$

where sigma is a solution to this Riccati ODE

$$\frac{d\sigma}{d\varphi} + (\iota_0 - N) \left[\frac{\bar{\eta}^4}{\kappa^4} + 1 + \sigma^2 \right] - \frac{2G_0\bar{\eta}^2}{B_0\kappa^2} \left[\frac{I_2}{B_0} - s_\psi \tau \right] = 0$$

here $\bar{\eta} = B_{1c}/B_{0}$, I_2 proportional to toroidal current on axis, $s_{\Psi} = sign(\Psi)$

Direct construction tool: inputs

- Fortran numerical tool constructs boundaries up to O((r/R)^2), allowing for shaping such as bean/triangular flux surfaces, Shafranov shift, and finite pressure profiles
- Input parameters: nfp, aspect ratio, R and Z axis Fourier coefficients, $\bar{\eta}$, B_{2c}, B_{2s}, I₂, p₂, σ (0)
 - $\bar{\eta}$ = B_{1c} / B₀ describes magnitude that B varies on a flux surface $B pprox B_0 \left[1 + r \bar{\eta} \cos \vartheta + O((r/\mathcal{R})^2) \right]$
 - I₂ toroidal current density on axis
 - B_{2c/s} how B varies with toroidal angle
 - p₂ determines pressure profile

$$\mathcal{I}(s) = 2\pi s a^2 I_2/\mu_0$$

$$p(r) \, = \, (1 - r^2/a^2) p_2$$

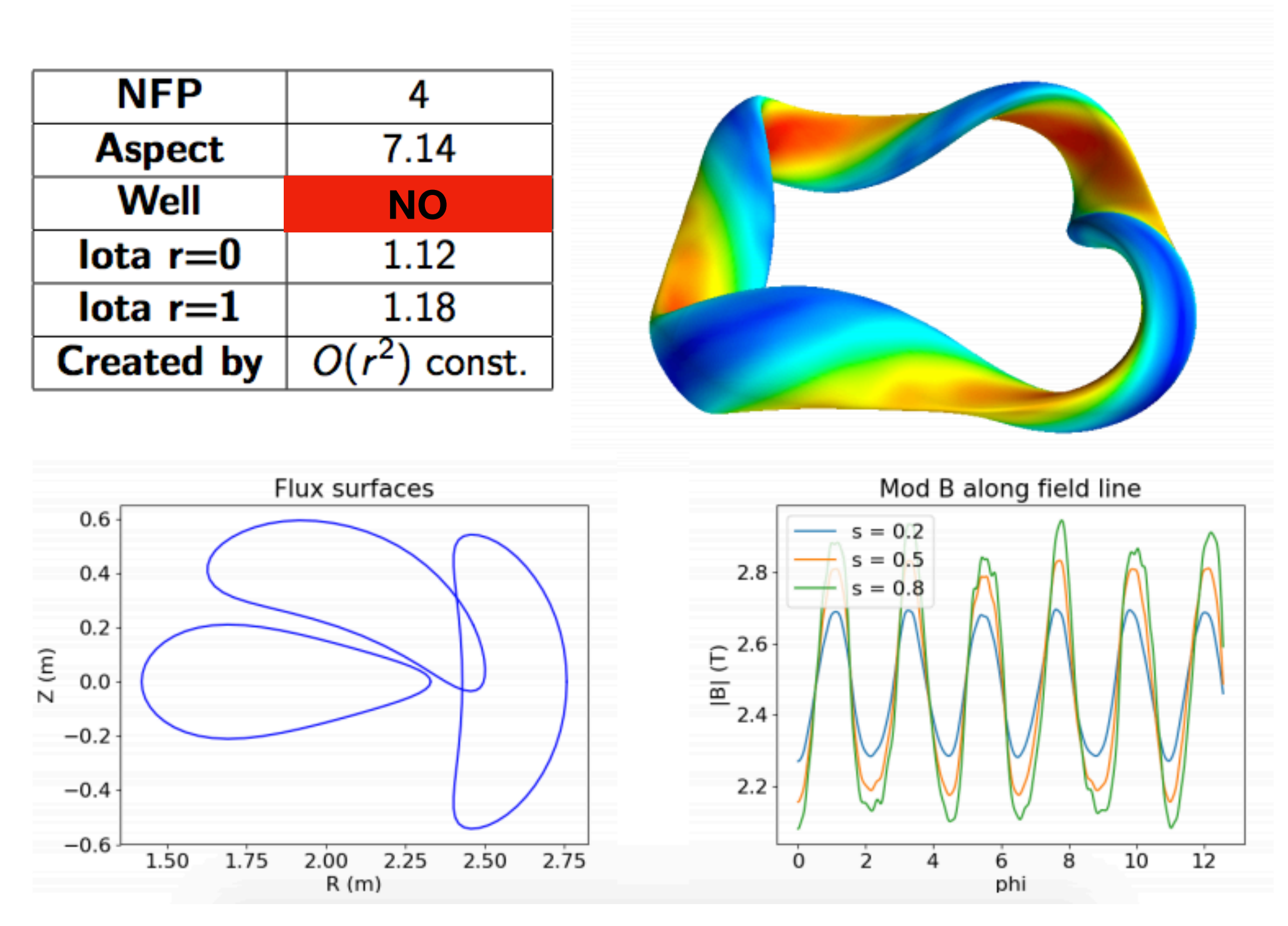
- $\sigma(0)$ is orientation of flux surface relative to normal vector of axis at $\phi = 0$
- For zero beta, stellarator symmetric configuration, many of these are set to zero B_{2s} , I_2 , $\sigma(0)$, R sine series, Z cosine series, p_2

Direct construction: outputs

- Output parameters of interest:
 - X, Y, Z expansion arrays magnitude of X₂,Y₂, X₃,Y₃, reflect quality of quasisymmetry (too large leads to self intersecting boundary)
 - iota on axis
 - magnetic well parameter on axis (d²V/dΨ², negative for stability)
 - max/mean elongation
 - B₂₀ residual i.e. deviation from constant magnetic field strength on axis
 - also axis length, max/mean curvature, torsion
- One way to access quality of solution is this objective:

$$f = w_{X2}\overline{(X_2 \cdot X_2)} + w_{Y2}\overline{(Y_2 \cdot Y_2)} + w_{X3}\overline{(X_3 \cdot X_3)} + w_{Y3}\overline{(Y_3 \cdot Y_3)} + w_{B20}(B_{20}_residual)$$

Constructed: mljs_2

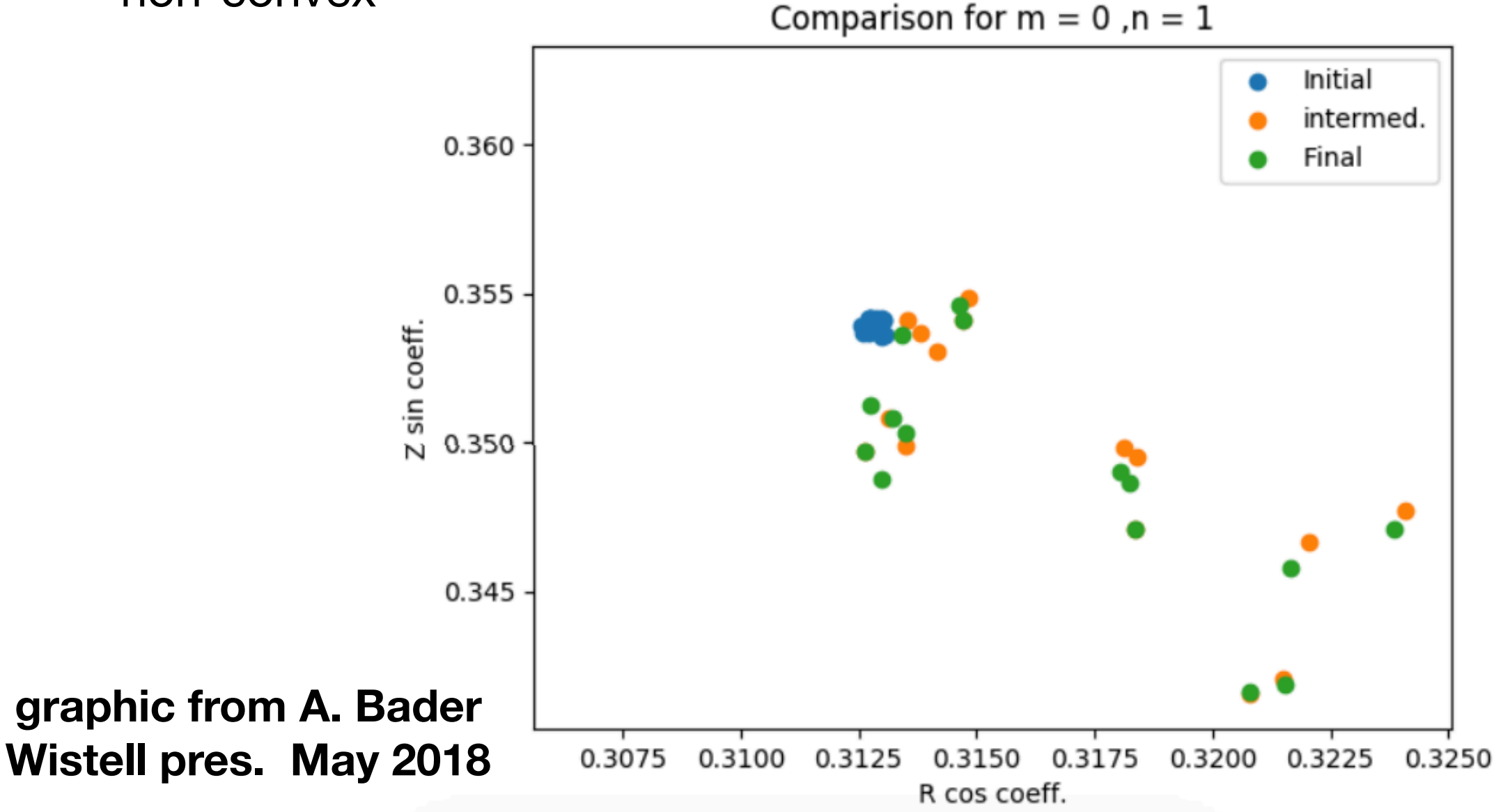


slide from Aaron Bader WISTELL presentation, 8/9/2019

 Reference to a 'found minima' or 'optimized solution' going forward in talk will be in reference to this solution

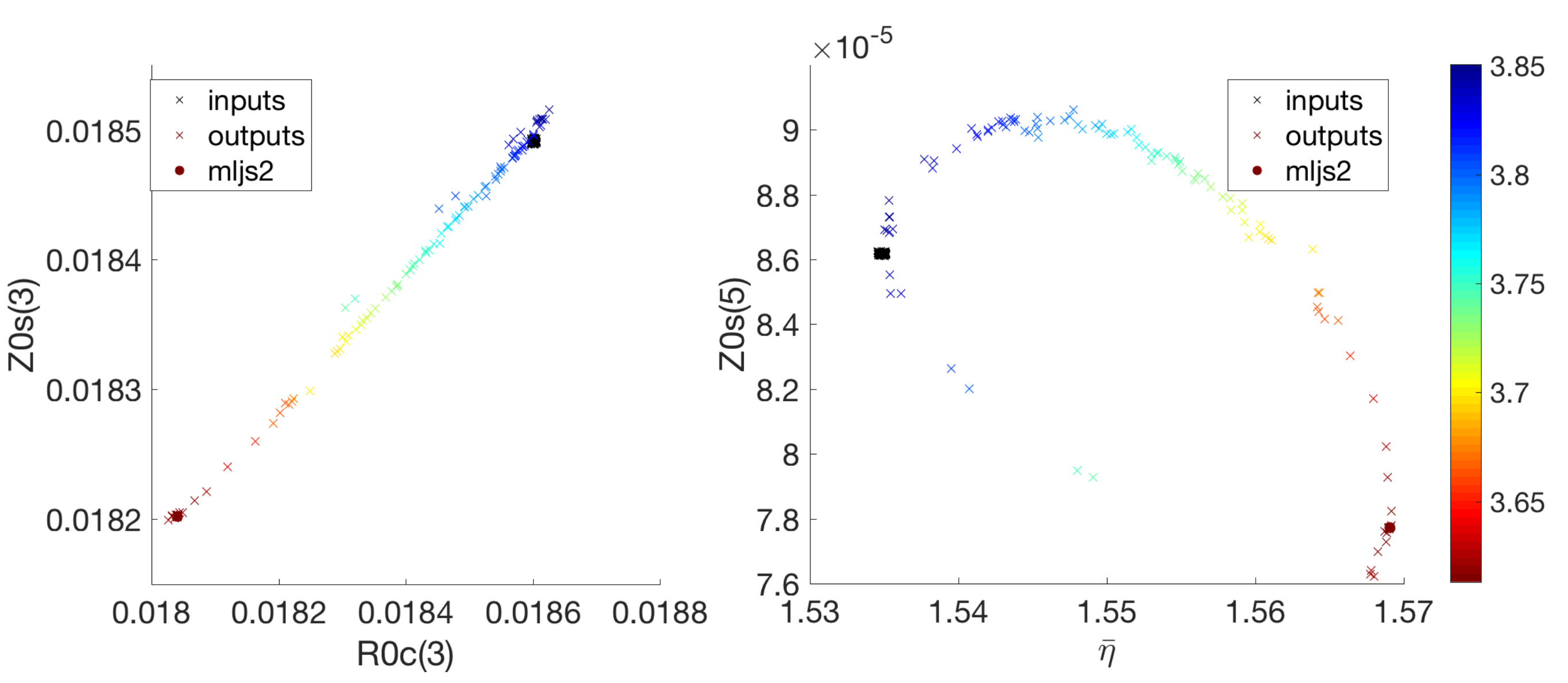
Optimization gives information about solution space

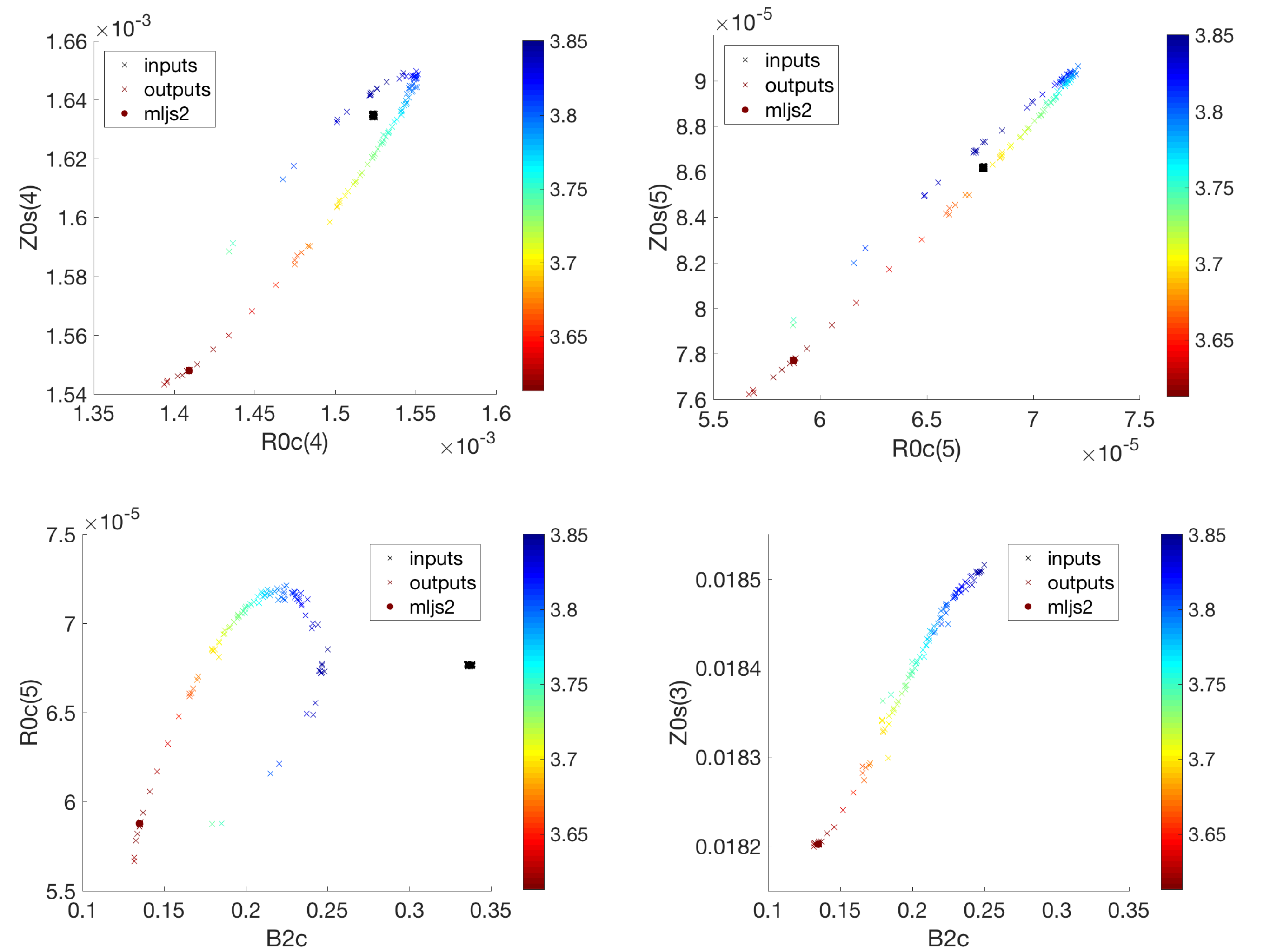
- Good QHS solutions appear to need a delicate balance in inputs
- Optimization can find be used to find solutions several previous Wistell candidate solutions were all found using a Nelder-Mead simplex method
- Aaron ran convexity scans on STELLOPT/ROSE and found the space to be non-convex



Optimization of input parameters yields curves in parameter space

- A small scan of optimization runs near a found minima shows that good solutions appear to lie in narrow valleys in parameter space
- Optimizer getting trapped in local minima is still an issue





Brute force parameter scan

- Alternative method is a direct parameter scan
- Multiple scans performed over a 10-D parameter space in the vicinity of an optimized solution
- Evenly spaced grid of length 5 over 10 dimensions (8 axis shape terms, eta_bar and B_{2c}) produces 5¹⁰ ~ 10 million solutions per scan
- Data produced and collected on CHTC system
- Plots produced with Vaex rapid plotting of massive sets made possible by visualizing heatmaps of averaged quantities

Local scan around optimized solution

 A parameter scan of values close around minima shows that solutions degrade quickly away from an optimized solution

parameter ranges:

Rc1: 0.16-0.18

Rc2: 0.017-0.019

Rc3: 0.001-0.002

Rc4: 0.00002-0.00008

Zs1: 0.15-0.165

Zs2: 0.017-0.019

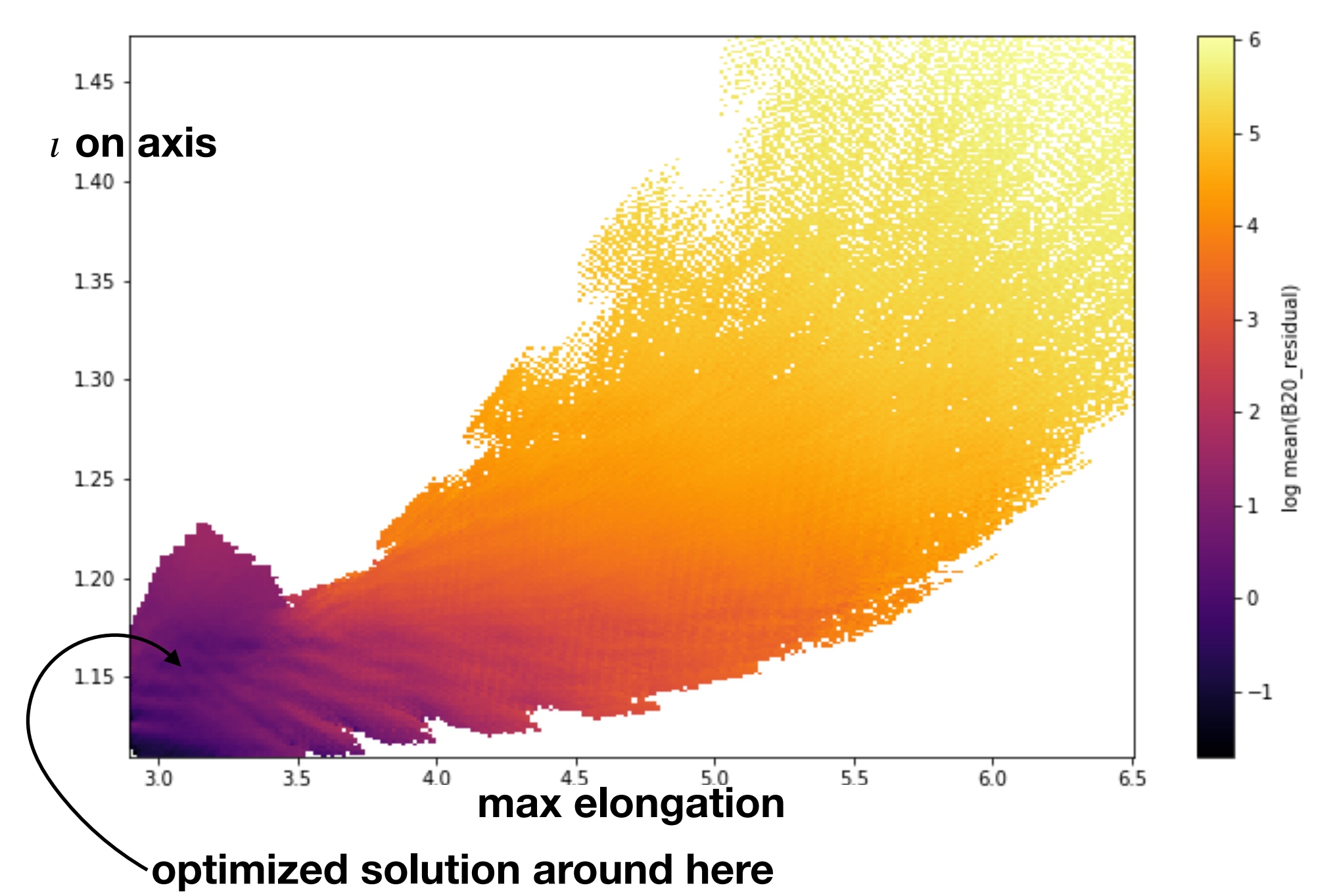
Zs3: 0.001-0.002

Zs4: 0.00003-0.00009

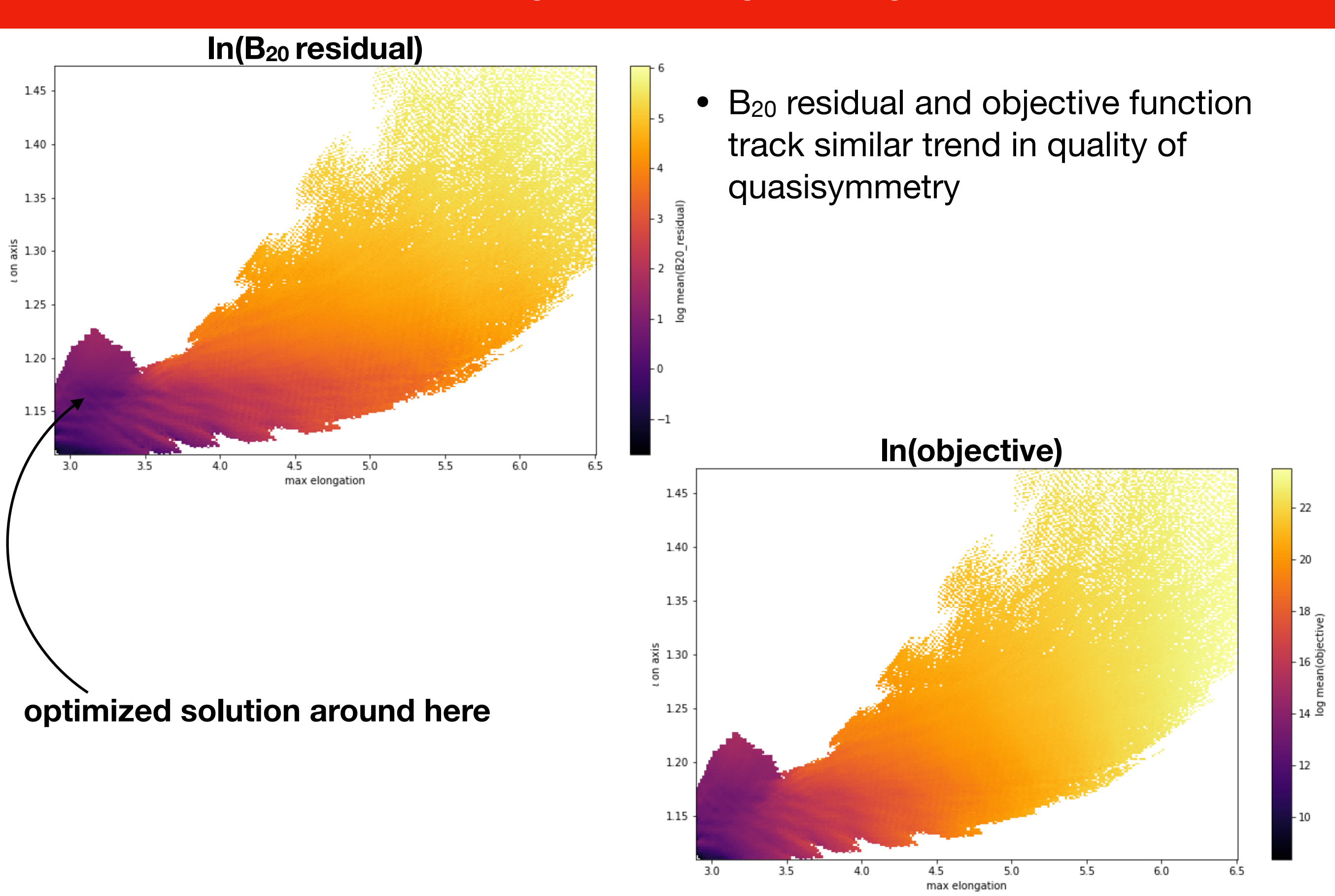
 $\bar{\eta}$: 1.565-1.575

B2c: 0.134-0.136

In(B₂₀ residual)

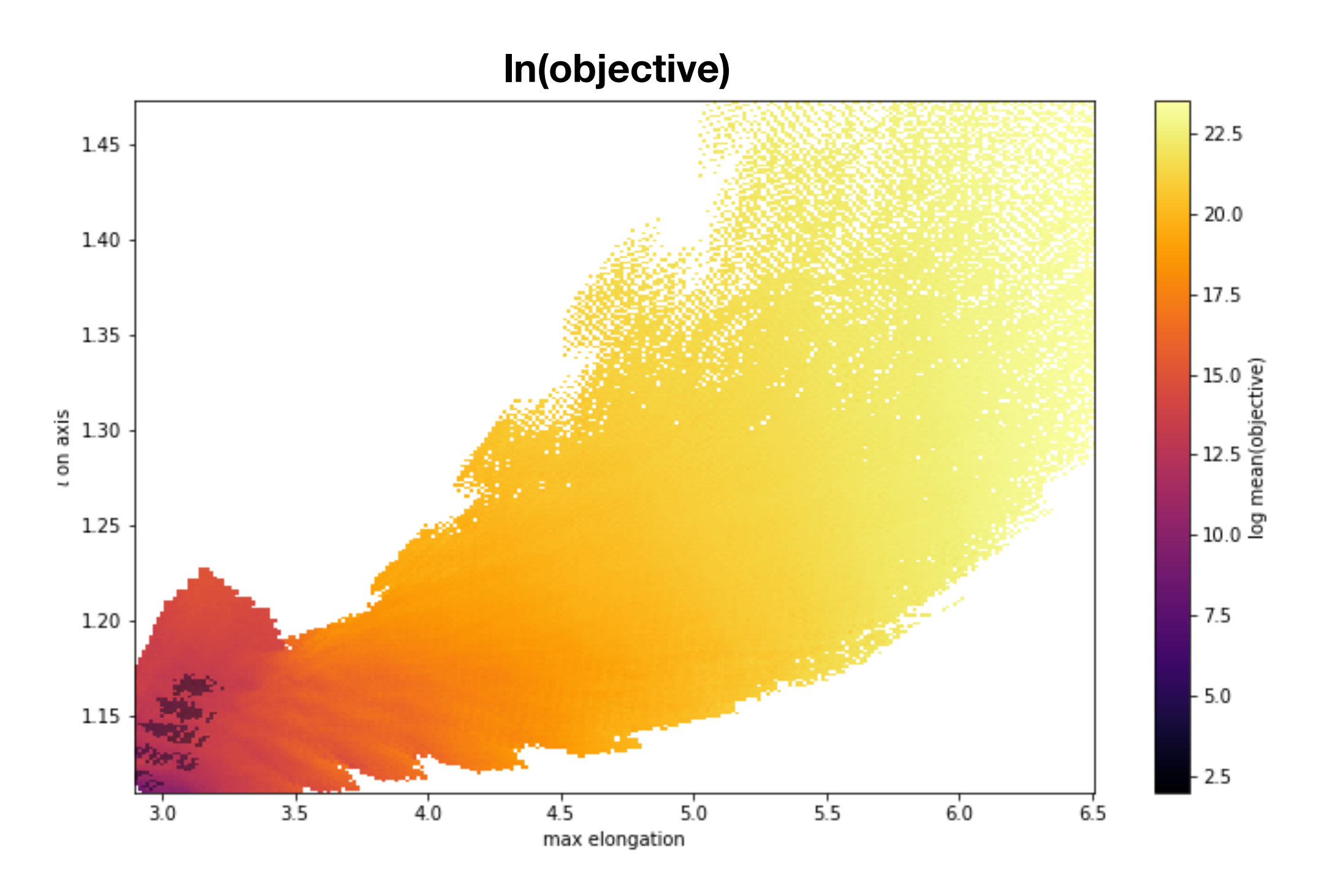


B₂₀ residual and objective function both indicative quality of quasisymmetry



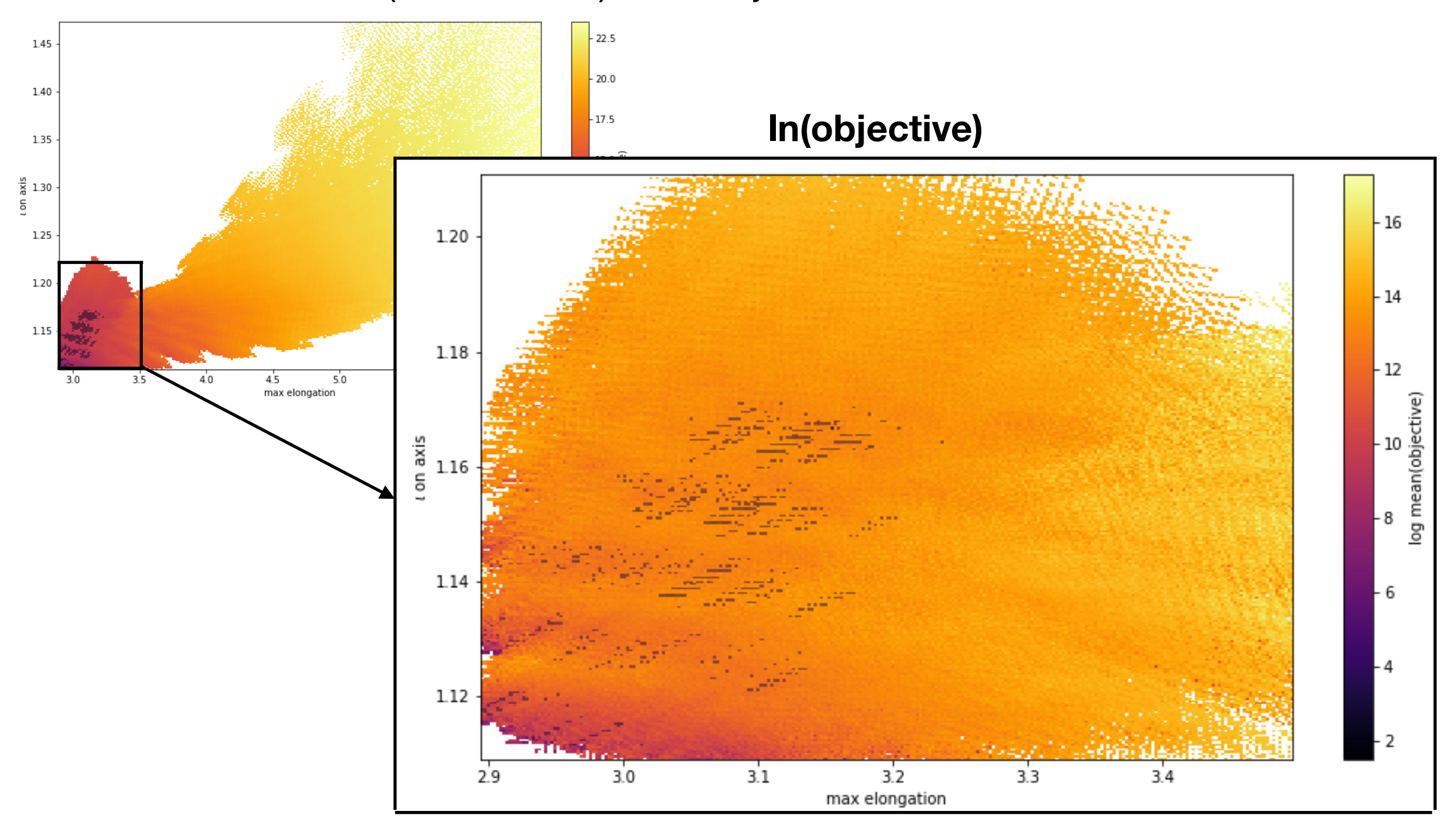
Point selection of best solutions

 Vaex allows for easy selection of points — below highlights a selection of all solutions (about 4400) with objective<50



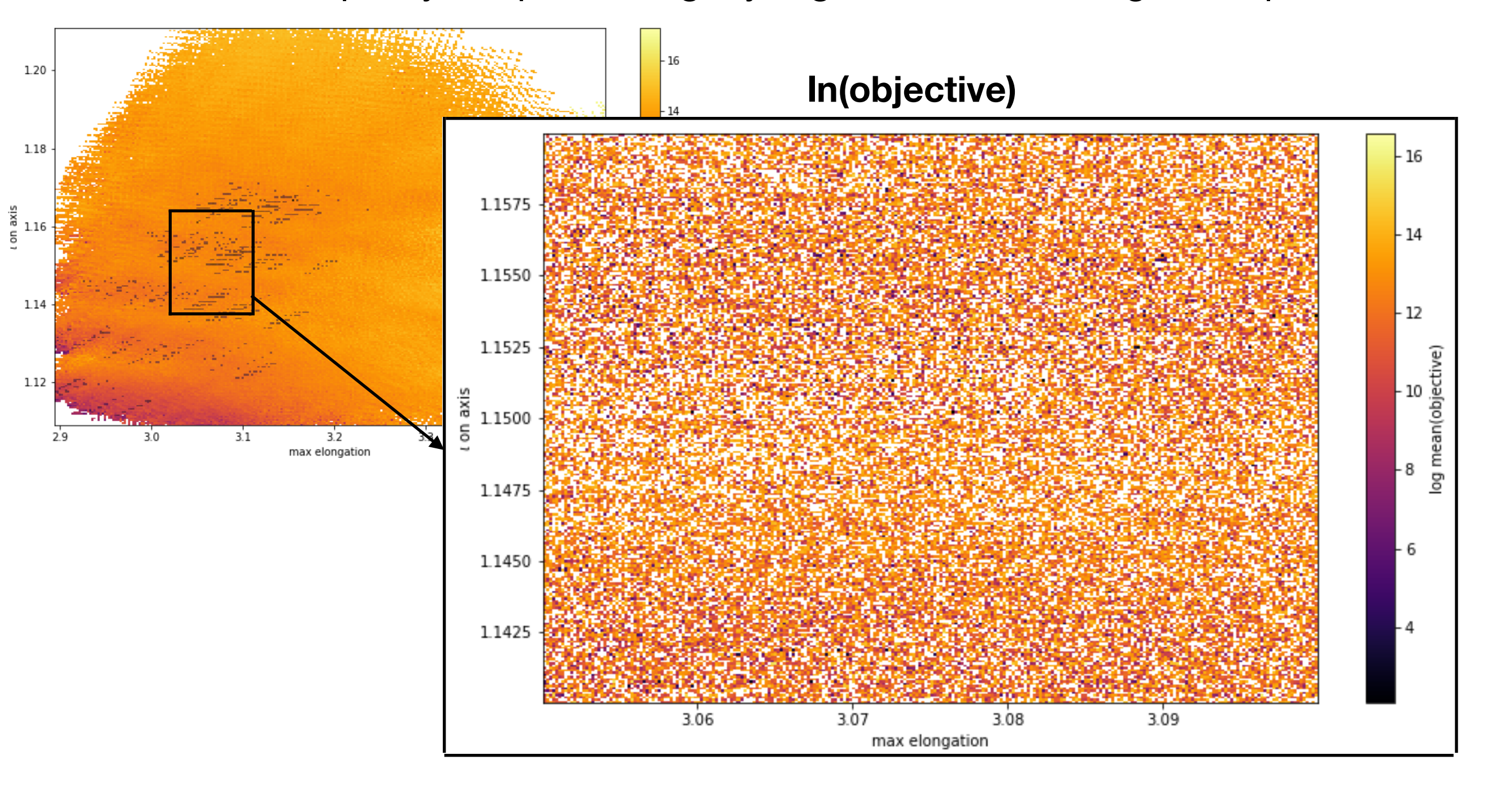
Best points cover small area in iota-elongation space

 Vaex allows for easy selection of points — below highlights a selection of all solutions (about 4400) with objective<50



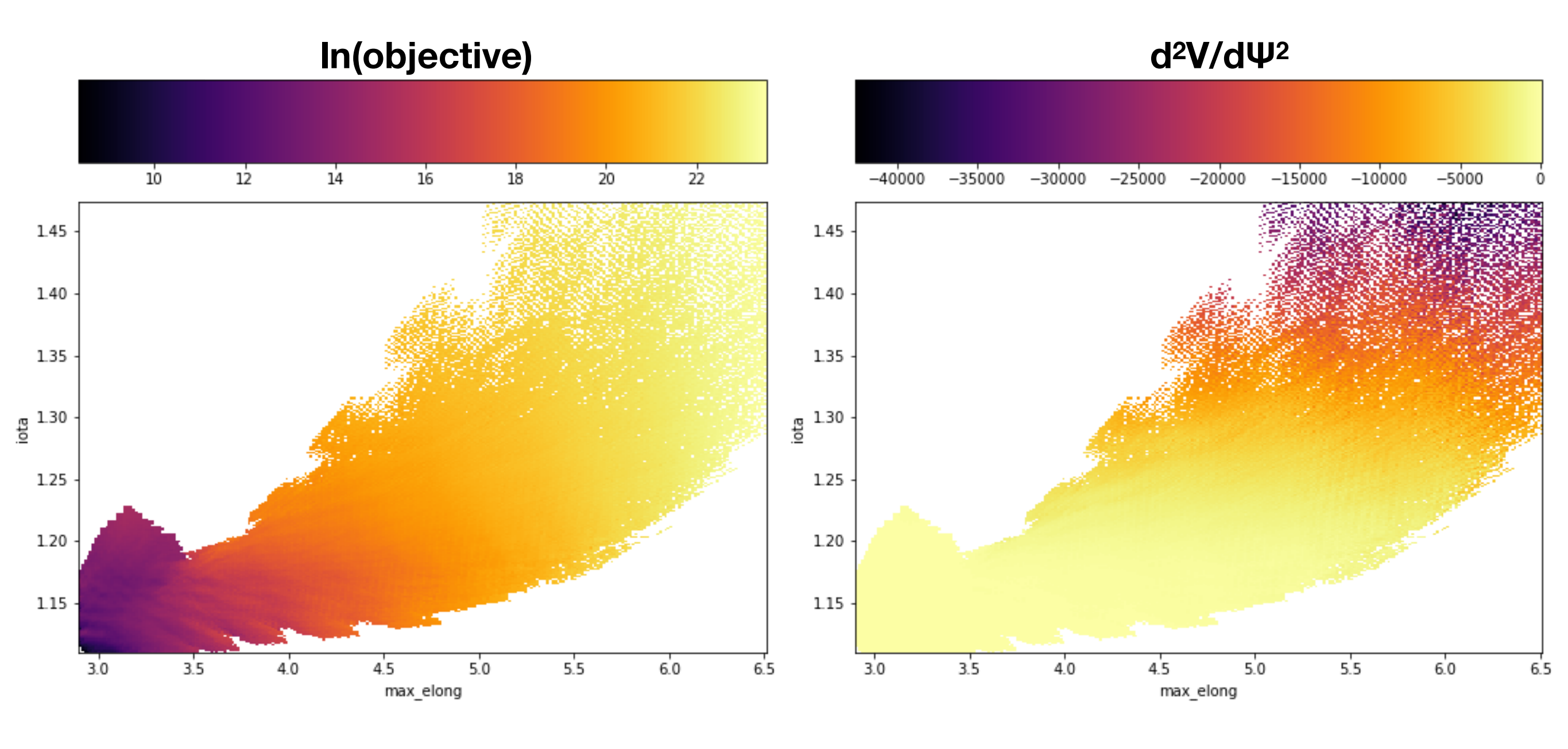
Solutions mixed throughout iota-elongation space

 Vaex plots heat map of mean quantities - this means information in large scale plots gets smoothed out, a lot of solutions with very different quality are packed tightly together in iota/elongation space



Objective and magnetic well inversely correlated in local scan

- At least locally, quality of quasisymmetry and presence of on axis magnetic well appear to be inversely correlated
- Recall for stability, $d^2V/d\Psi^2 < 0$



Broader scan around optimized solution

 A parameter scan of values near close around minima shows that solutions degrade quickly away from an optimized solution

parameter ranges:

Rc1: 0.14-0.20

Rc2: 0.012-0.022

Rc3: 0.0008-0.0022

Rc4: 0.00001-0.0001

Zs1: 0.13-0.19

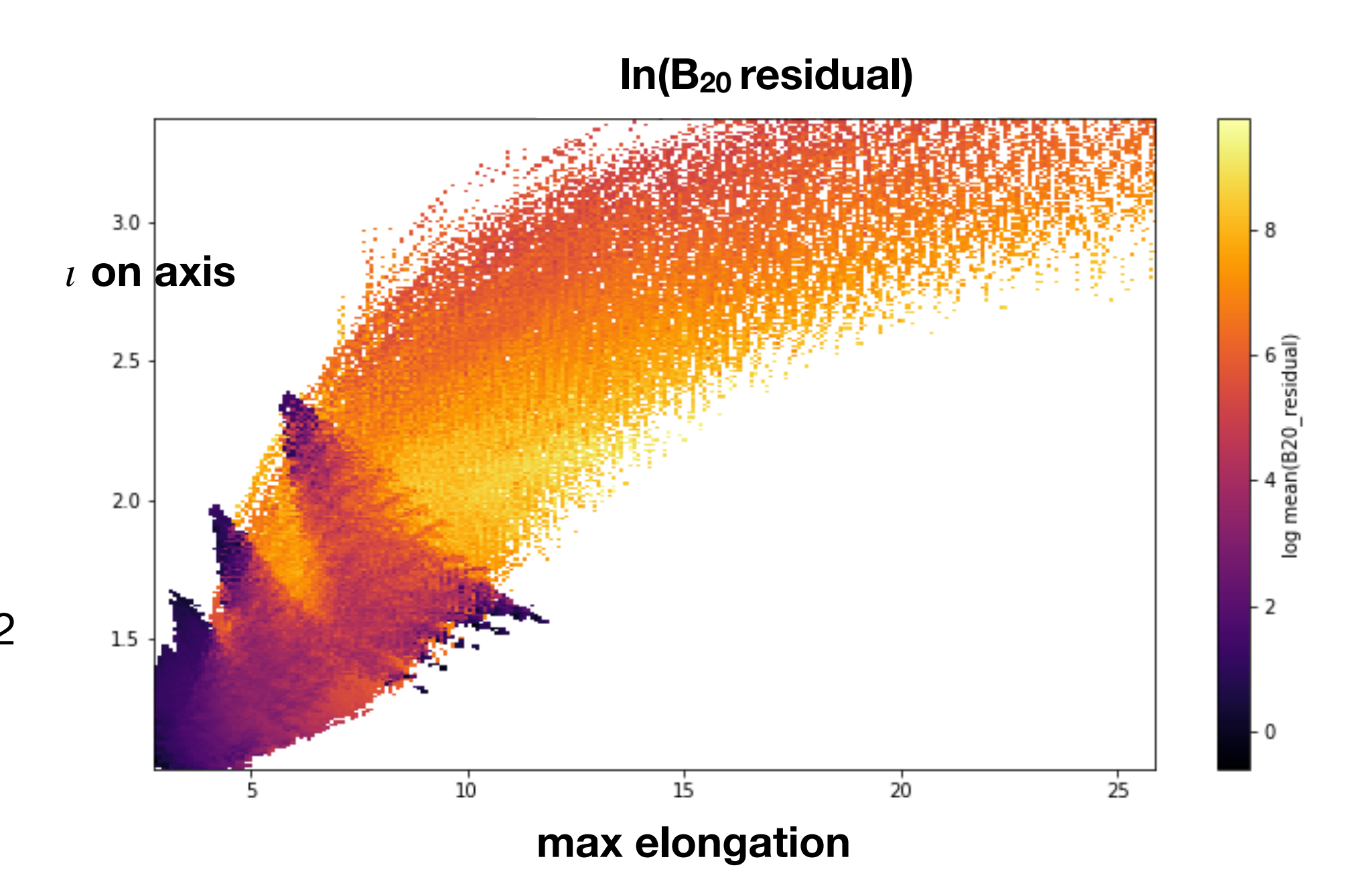
Zs2: 0.014-0.022

Zs3: 0.0006-0.0024

Zs4: 0.00001-0.00012

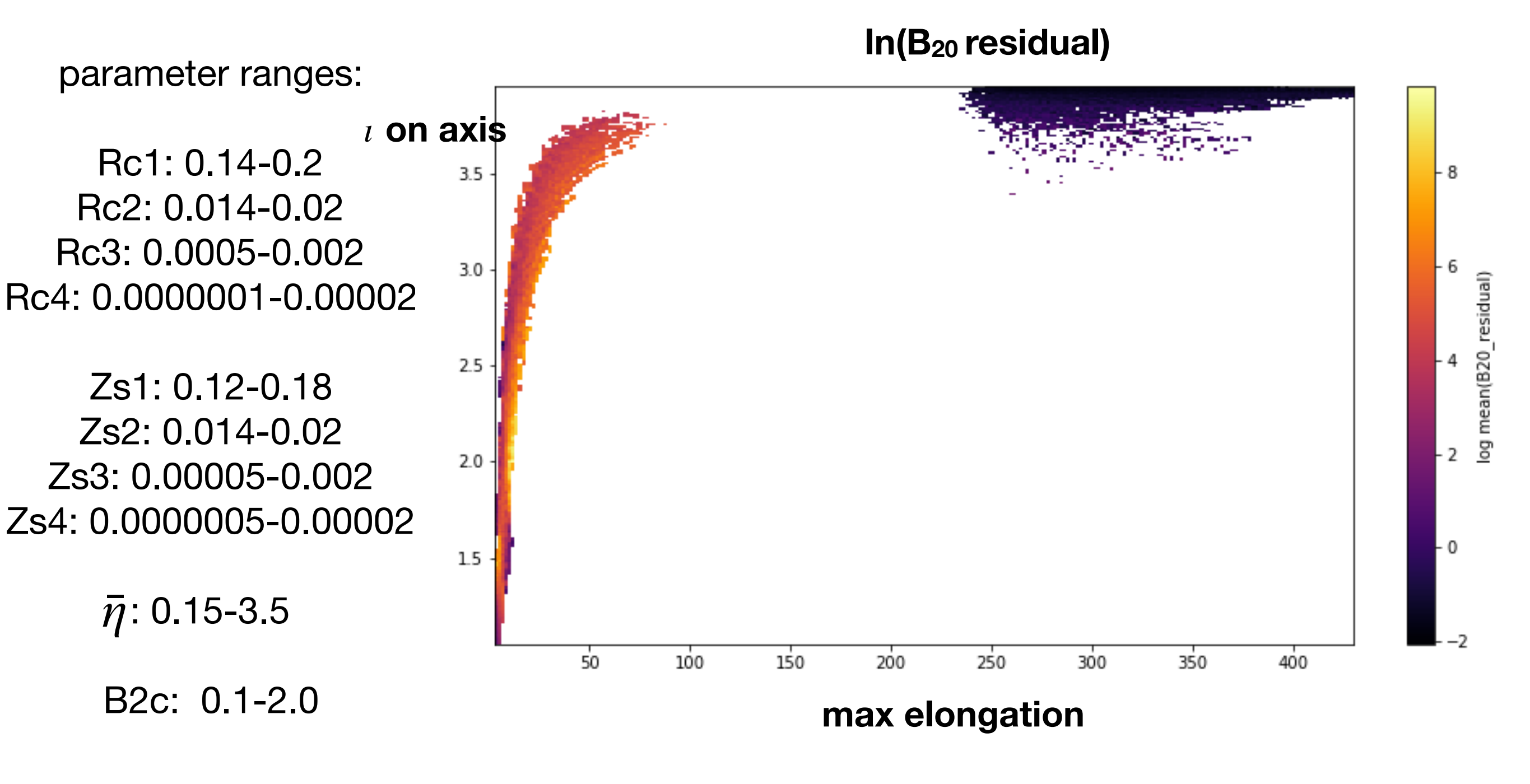
 $ar{\eta}$: 1.0-1.8

B2c: 0.1-0.6



Scan broad in non-axis parameters

 Broader scan shows many solutions at incredibly high elongation, but also a higher range of iota values at lower elongation



Selection of low elongation solutions looks qualitatively similar to other scans

- "Zooming in" on just the low elongation solutions, the chart looks more like the scans seen before
- Biggest difference is the higher range in on axis iota values

parameter ranges:

Rc1: 0.14-0.2

Rc2: 0.014-0.02

Rc3: 0.0005-0.002

Rc4: 0.000001-0.00002

Zs1: 0.12-0.18

Zs2: 0.014-0.02

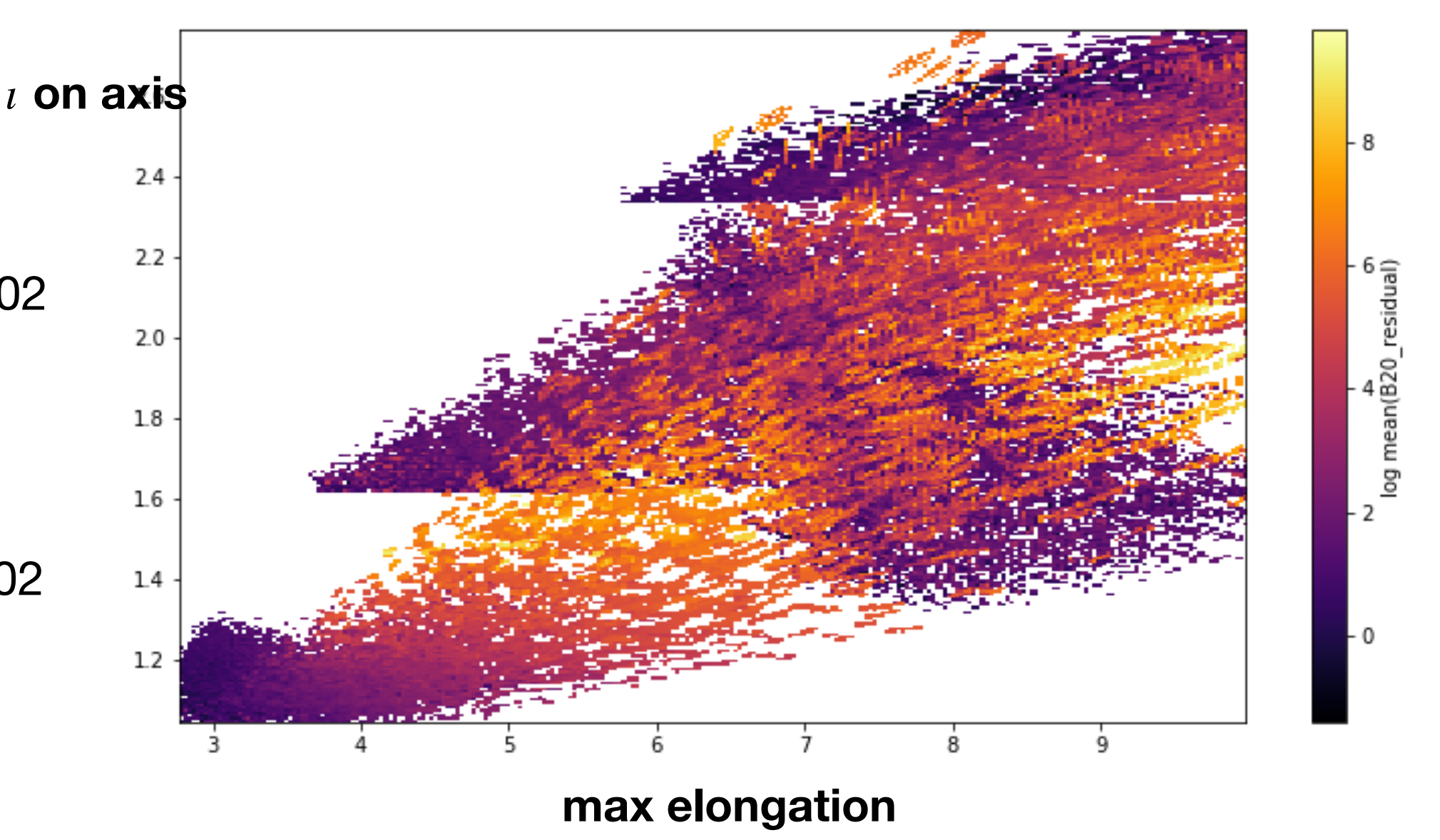
Zs3: 0.00005-0.002

Zs4: 0.0000005-0.00002

 $\bar{\eta}$: 0.15-3.5

B2c: 0.1-2.0

In(B₂₀ residual)



Conclusions

- Good solutions to direct construction tool appear to lie on curves in multidimensional parameter space, as found using Nelder-Mead optimization
- When parameters are varied in a regular way away from that curve, as done for the parameter scans shown today, solutions degrade very quickly

Ideas for next steps

- More informed parameter scans/further analysis of parameter scans already performed
 - Arrange Fourier axis modes such that same order R/Z terms are comparable in magnitude
- Perform course scans with use of Nelder-Mead method at each grid point, rather than simple evaluation of inputs over a large grid
 - Possible room for improvement in optimization scheme
- Perform conventional optimization procedures on found solutions
- Extend work to other number of field periods several minima have been found previously for 5 field period configurations
- Extend work to finite beta configurations for all work here $p_2 = 0$